Excitation–Emission Matrix Fluorescence Spectroscopy for Natural Organic Matter Characterization: A Quantitative Evaluation of Calibration and Spectral Correction Procedures

R. DAVID HOLBROOK,* PAUL C. DEROSE, STEFAN D. LEIGH, ANDREW L. RUKHIN, and N. ALAN HECKERT

Surface and Microanalysis Science Division, National Institute of Standards and Technology, Gaithersburg, Maryland 20899 (R.D.H.); Biochemical Science Division, National Institute of Standards and Technology, Gaithersburg, Maryland 20899 (P.C.D.); and Statistical Engineering Division, National Institute of Standards and Technology, Gaithersburg, Maryland 20899 (S.D.L., A.L.R., N.A.H.)

The influence of different data collection procedures and of wavelength-dependent instrumental biases on fluorescence excitation–emission matrix (EEM) spectral analysis of aqueous organic matter samples was investigated. Particular attention was given to fluorescence contours (spectral shape) and peak fluorescence intensities. Instrumental bias was evaluated by independently applying excitation and emission correction factors to the raw excitation and emission data, respectively. The peak fluorescence intensities of representative natural organic matter and tryptophan were significantly influenced by the application of excitation and emission spectral correction factors and by the manner in which the raw data was collected. Humification and fluorescence indices were also influenced by emission correction factors but were independent of reference (excitation) intensity normalization or correction. EEM surface contours were dependent on normalization of the fluorescence intensity to the reference intensity but were not influenced by either excitation or emission spectral correction factors. Authors should be explicit in how excitation and emission spectral correction procedures are implemented in their investigations, which will help to facilitate intra-laboratory comparisons and data sharing.

Index Headings: **Calibration; Fluorometers; Natural organic matter; Peak intensity; Peak location; Spectral correction.**

INTRODUCTION

Fluorescence excitation–emission matrix (EEM) spectroscopy is a powerful and widely used technique for characterizing the heterogeneous composition of fluorescent organic matter normally found in both affected and natural aqueous environments.[1,2] This method entails collection of emission spectra at multiple excitation wavelengths, producing a topographic or contour plot where the excitation and emission coordinates of observable fluorescence peaks can be used to help identify different fluorophore moieties. Prevalent fluorophore moieties in natural waters that have been identified by EEM include humic and fulvic acids[3–5] and aromatic proteins.[2] Detection of environmental pollutants at parts-per-billion to parts-per-trillion levels have also been demonstrated.[6] While only a small fraction of aromatic species actually emit light[7] and are therefore detectable by fluorescence spectroscopy, the advantages of EEM, which include small sample volume (e.g., 10 mL), minimal sample preparation (e.g., 0.45 μm filtration), and quick analysis time (e.g., between 10 minutes to 20 minutes per sample), make this technique an attractive candidate for both routine and intensive monitoring/screening of natural systems.

Individual fluorescence spectra can be significantly altered by environmental conditions. For example, sample pH,[8] metals,[9] and ambient temperature can all influence fluorophore behavior, and fluorescence spectra must be corrected for primary and secondary inner filter effects for samples with high turbidity.[8,10] The majority of investigations available in the literature either report, control, or correct for these ambient conditions. However, fluorescence spectra will also include instrumental bias,[11] which results in systematic errors in the measured fluorescence intensity caused by the wavelength-dependent output or response of individual instrument components, such as excitation lamps, monochromator gratings, and detectors. The amount of instrumental bias will vary among different instruments, thereby making comparisons of fluorescence spectra collected from different laboratories unfeasible unless the bias is first removed through calibration and applying correction factors to both excitation and emission spectra.[12] It is important to note that EEM data collected on a single instrument and not corrected for instrument bias are internally comparable, signifying that calibration and spectral correction factors may not be necessary in all applications. However, as we demonstrate in this work, elimination of instrument bias can improve the accuracy of fluorophore detection, especially at low excitation and emission wavelengths, where the fluorometer sensitivity may be diminished.

Arguably, removal of instrumentation bias during EEM investigations is more important than during conventional fluorescence spectroscopy (e.g., collection of a single emission spectrum) because measurements are dependent on both excitation and emission wavelengths: correction factors are a product of two numbers instead of one. Due to the large quantity of individual data points in each EEM (often between 2000 and 10 000 individual measurements), fluorophore characterization is often reduced to the excitation and emission wavelength coordinates and fluorescence intensity[2] of any observable peaks. More recent techniques, such as fluorescence regional integration[3] and multivariate modeling,[13,14] make use of the entire EEM and arguably provide a more robust description of complex fluorophore moieties. Any EEM analysis technique relies on spatial variations of fluorescence intensity, and is therefore influenced by the intensity magnitude and physical location (described by excitation and emission coordinates) of any peak(s). Consequently, inaccurate quantification of the fluorescence intensity or the location within the matrix may result in an erroneous description.

In this work, we investigate the importance of excitation and emission correction factors during EEM investigations of organic matter in aqueous samples. EEM results of representative International Humic Substance Society (IHSS) samples

Received 3 February 2006; accepted 1 May 2006.
* Author to whom correspondence should be sent. E-mail: dave.holbrook@nist.gov.

0003-7028/06/6007-0791$2.00/0

(natural organic matter (NOM), humic acid, and fulvic acid) and a surrogate compound representative of organic matter found in wastewater effluents[1] (tryptophan) were compared. Our results indicate that removal of instrumental bias improves fluorophore resolution (i.e., peak location and intensity) and can make a qualitative, as well as a quantitative, difference in experimental results. In addition, proper instrument calibration will facilitate intra-laboratory comparisons and data sharing of EEM data.

EXPERIMENTAL

Fluorescence Material: Source and Sample Preparation. Rhodamine B (RhB), Rhodamine 101 (Rh101), and 9,10 diphenylanthracene (DPA) were used as quantum counters to compare their behavior in the 200 nm to 400 nm spectral region to each other as well as to the reference photodiode, or R channel. RhB was obtained from Eastman, Rh101 from Exciton, and DPA from Aldrich, and each were used without further purification. Solutions of RhB and Rh101 were prepared in ethanol at concentrations of 5 mg/L, while a 1 mg/L solution of DPA was prepared in cyclohexane. Three organic matter reference materials were obtained from the IHSS, including Nordic aquatic humic acid (NAHA), Suwannee River fulvic acid (SRFA), and Suwannee River natural organic matter (SRNOM). The fourth organic matter reference material, tryptophan, was obtained from Fisher Scientific. Stock solutions of the IHSS materials were prepared by dissolving a known mass of each substance in Milli-Q water (Millipore, Bedford, MA), bath sonicating for 10 minutes, and mixing on a stir plate for 24 hours. Aliquots of the stock solution were combined with Milli-Q water to produce working samples with a final concentration of 50 mg/L (as dry weight). Stock solutions of tryptophan were produced in a similar manner, although bath sonication was not used and the working samples had a final concentration of approximately 10 μg/L. A biphasic solution of NAHA and tryptophan was produced by mixing the two stock solutions together and diluting with Milli-Q water to a final concentration of 40 mg/L and 20 μg/L, respectively. The working solutions were used in the excitation–emission matrix fluorescence spectroscopy investigations. All solutions were stored in the dark at 4 °C and discarded after 2 weeks.

Excitation–Emission Matrix and Conventional Fluorescence Spectroscopy. Excitation–emission matrices were collected on a SPEX Fluorolog 3 (Horiba Jobin Yvon, Edison, NJ) with a continuous 450 W Xe lamp light source, double monochromators for selection of both excitation (gratings blazed at 330 nm) and emission (gratings blazed at 500 nm) wavelengths, and an R928-P (Hamamatsu, Bridgewater, NJ) photomultiplier tube (PMT) for detection of emission intensity, referred to as the signal intensity (S). A small fraction of the excitation beam is diverted to a silicon (Si) photodiode just before the sample using a fused silica window to measure the relative intensity of the excitation light, and this portion of the beam is referred to as the reference intensity (R). Aliquots of the aqueous solutions containing the organic matter were transferred into a standard rectangular fluorometric cuvette (Fisher Scientific, Pittsburg, PA), made of far-UV grade quartz and having a 1 cm path length, and the sample's fluorescence was collected at 90 degrees from incidence. Uncorrected and reference intensity corrected signal intensities, S and S/R, were monitored and saved as a function of both excitation and emission wavelengths, which are individually scanned from 200 nm to 400 nm in 5 nm increments and from 300 nm to 500 nm in 2 nm increments. The excitation and emission bandwidths were both set at 5 nm and the integration time at each wavelength pair was 0.3 seconds. The water Raman peak (348 nm/397 nm) of distilled water was collected before each EEM experiment to monitor instrument stability.[1] We observed no appreciable variation in the water Raman peak intensity (coefficient of variation $<3\%$) during the investigation. Absorbance measurements of each sample were collected between 200 nm and 500 nm using a Perkin-Elmer Lambda 900 spectrophotometer and were used to correct each EEM for both primary and secondary inner filter effects (IFE)[8] using the relationship developed by MacDonald et al.[15] Raman scattering effects were removed by subtracting an IFE-corrected EEM of distilled water from the IFE-corrected EEM of the individual samples. Finally, the fluorescence intensity scale for all spectra was normalized to the water Raman peak intensity. The resulting EEMs were plotted with SigmaPlot (Version 8.02, Chicago, IL) using 20 equal intensity contour lines.

Each of the organic dye solutions used as quantum counters were put in a quartz cuvette placed at the sample position with the excitation beam at normal incidence. The excitation spectrum for each solution was collected between 200 nm and 400 nm at a fixed emission wavelength. The emission wavelength used for RhB and Rh101 was either 750 nm or 810 nm and for DPA was either 400 nm or 500 nm. The fluorescence from each quantum counter was collected at an angle of 22° with respect to the excitation beam using a front face geometry. The excitation and emission bandwidths were both set to 5 nm and the integration time was 0.5 s. At the dye concentrations used, the penetration depths of the excitation beam before being totally absorbed is small, approximately 1 mm to 2 mm.

Excitation–Emission Matrix Spectral Correction. The correction factors for R were determined using a calibrated detector (CD) at the sample position to measure the excitation intensity as a function of wavelength from 200 nm to 400 nm. The correction factors for S were determined using a calibrated light source (CS)-based method for emission wavelengths from 370 nm to 500 nm, and a CD-based method for emission wavelengths from 280 nm to 370 nm, to measure the response of the detection system as a function of emission wavelength. The CS-based method is a one-step method that uses a calibrated reflector (CR) at the sample position to reflect the light from the CS into the detection system. The CD-based method is a two-step method, in which the CD was used to measure the excitation lamp intensity as a function of wavelength in the first step, just as was done for determining the R correction, and in the second step the CR was placed at the sample position to reflect the excitation light into the detection system. The CD, the CR, and the CS were previously calibrated for spectral responsivity, reflectance, and radiance, respectively, in the NIST Physics Laboratory and are traceable to the SI.

The R correction factors $C_R(\lambda)$ were calculated by dividing the corrected excitation source intensity measured by the CD at the sample position ($I_{CD}(\lambda)$) by the R channel intensity ($R_{CD}(\lambda)$), measured simultaneously (Eq. 1). The corrected reference intensity $R_{cor}(\lambda)$ was then calculated using Eq. 2:

$$C_R(\lambda) = I_{CD}(\lambda)/R_{CD}(\lambda) \quad (1)$$

$$R_{cor}(\lambda) = C_R(\lambda)R(\lambda) \quad (2)$$

where $R(\lambda)$ is the R channel intensity of the sample. S correction factors $C_S(\lambda)$ were calculated using S, R, and I_{CD} intensities measured during the implementation of the S calibration methods, enabling the corrected signal intensity to be calculated using Eq. 3:

$$S_{cor} = C_S(\lambda)S \quad (3)$$

A detailed explanation of the measurements and calculations involved in determining C_S using both CS-based and CD-based methods is given elsewhere.[16] The CS-based method was used because it was found to have smaller uncertainties than the CD-based method in the visible region of the spectrum under our experimental conditions. Below 370 nm, the output of the tungsten CS became very weak, requiring the use of the CD-based method in this region. When spectral correction factors are applied to the collected raw data, the subscript "cor" is used (e.g., S_{cor}/R_{cor}).

Statistical Analysis. Statistical comparison between corresponding EEM data was performed by two methods in order to evaluate the impact of the data collection procedure (i.e., S versus S/R) and use of the EEM correction factors on (1) spectral shape and (2) peak fluorescence intensity. The form of spectral shape analysis used first computes the correlation coefficient (r) between individual excitation spectra for matching emission wavelength between two EEM matrices. These individual r values, along with the bootstrapped[17] estimates of error for each excitation/emission wavelength pair, are then plotted against the indexing emission wavelength to determine whether there are any consistent deviations from correlation unity as a function of emission wavelength between different samples. Consistent correlation values close to 1.0 across the range of emission wavelengths provide a strong indication of insignificant changes between the two corresponding EEM datasets. This can be tested formally using a null hypothesis of the form

$$H_0 : \rho_0 \leq \rho \leq 1.0 \quad (4)$$

This test is implemented by comparing the individual empirical r values to the test statistics (r_0):[18]

$$r_0 = \frac{(1+\rho_0)e^{2z_\alpha/\sqrt{n}} - (1-\rho_0)}{(1+\rho_0)e^{2z_\alpha/\sqrt{n}} + (1-\rho_0)} \quad (5)$$

where ρ_0 is the user-defined lower acceptable correlation coefficient (0.90 was used in this investigation), z_α represents the critical point of the standard normal (e.g., for $\alpha = 0.05$, $z_\alpha = -1.68$), and n, which should be at least 20, is the number of non-zero matched values in the individual excitation spectra that are being correlatively compared. The null hypothesis is rejected when r is less than r_0. The p-value associated with this test can be computed approximately as[17]

$$\Phi\left[\sqrt{n}/2\log\frac{(1+r)(1-\rho_0)}{(1-r)(1+\rho_0)}\right] \quad (6)$$

where Φ represents the standard normal cumulative distribution function. This hypothesis testing machinery leads to a formally valid method for assigning a figure of merit to a test of similarity of structure between excitation spectra at each emission wavelength. The individual p-values provide a one-number goodness-of-fit summary to the match between an ideal correlation curve ($r = 1.0$) and the empirical correlation curve at the individual emission wavelength. To combine the one-number summary at each wavelength across the entire emission spectrum, one can combine p-values using Fisher's sum of log's method as follows:[18]

$$-2\sum_{i=1}^{k}\log(p_i) \quad (7)$$

where i indexes the emission wavelength and the individual p_i are the p-values computed at each of the wavelengths as described above. This aggregate test statistic is compared with the $100(1-\alpha)$ percent critical value of the chi-square distribution with 2000 degrees of freedom.

A second statistical evaluation compares the magnitudes of the water Raman peak-normalized intensity at specific excitation/emission wavelength pairs using the student's t-test (SigmaPlot 9.0, Chicago, IL). The excitation/emission wavelength pairs of the primary and secondary (if applicable) peak fluorescence intensity locations were identified from the S_{cor}/R_{cor} EEM plots and are summarized in Table I.

Calculated Indices. Humification (HI) and fluorescence (FI) indices were calculated from the IFE-corrected Raman normalized EEM data according to the methods proposed by Ohno[10] and McKnight et al.,[4] respectively.

RESULTS AND DISCUSSION

Evaluation of Spectral Correction Factors. The R correction curves obtained using the CD and quantum counters shown in Fig. 1 all have similar shapes with no disagreement greater than ±5% at any excitation wavelength from 300 nm to 400 nm. However, the quantum counters show a negative bias compared to the CD of as much as −20% below 300 nm. Typical deviations from flatness of the spectral response of such quantum counters has been reported to be about ±5%,[19] so it is likely that the greater deviations we observed can be minimized by optimizing the experimental setup to eliminate systematic errors due to scattered light, polarization effects, self-absorption, and differences in the optical path between the quantum counter and the sample. The reference photodiode (R channel) displays much larger deviations compared to the CD with a −43% bias at 280 nm and a +15% bias at 400 nm, demonstrating that uncorrected quantum counters are a better choice for reference intensity correction than an uncorrected Si photodiode for wavelengths less than 400 nm. The R channel bias is most likely due to the photodiode response, assuming the manufacturer minimized systematic errors when designing and aligning the instrument. In either case, the bias observed for both the photodiode and the quantum counters can be corrected using the CD data.

The quantum counters have measurable intensity all the way down to 200 nm, whereas the R channel gave an undetectable response below 225 nm (Fig. 1, inset). Therefore, fluorometers that use a Si photodiode R channel to monitor the variation in lamp reference intensity may be unable to accurately measure fluorescence intensities for excitation wavelengths below 250 nm and may have no response below 225 nm. Additionally, signal-to-noise ratios must be closely evaluated at low excitation wavelengths due to the relatively low lamp intensity output (Fig. 2, inset) combined with the low throughput of conventional monochromators in this region, regardless of how the R correction curves are obtained. The signal-to-noise ratio

TABLE I. Summary of fluorescence peak locations and their wavelength biases[a] for Figs. 4A through 4F.

	S	S_{cor}	S/R	S_{cor}/R	S/R_{cor}	S_{cor}/R_{cor}
Primary peak[b]						
Excitation (nm)	no peak	no peak	+1	+23	0	240
Emission (nm)	no peak	no peak	−5	+9	−5	448
Fluorescence intensity (RU)	no peak	no peak	+9.5	+3.4	+2.8	18.9
Secondary peak[b]						
Excitation (nm)	+20	+20	shoulder	shoulder	+5	325
Emission (nm)	+4	+4	shoulder	shoulder	+2	452
Fluorescence intensity (RU)	−0.9	−2.3	shoulder	shoulder	+1.6	11.6
Tertiary peak[c]						
Excitation (nm)	no peak	shoulder	shoulder	+1	−2	280
Emission (nm)	no peak	shoulder	shoulder	+5	+27	348
Fluorescence intensity (RU)	no peak	shoulder	shoulder	+9.2	−0.8	12.0

[a] Biases are all relative to S_{cor}/R_{cor}.
[b] Caused by NAHA.
[c] Caused by tryptophan.

was greater than 120:1 at the low excitation wavelengths (between 230 nm and 250 nm) for the NOM samples, which was deemed adequate.

Note that our photon counter gave an intensity proportional to the number of photons incident on it, while the reference photodiode gave an intensity proportional to the power of the incident light. Relative power units were converted to relative photon units in Fig. 1 for R and CD by multiplying by the wavelength. All the curves shown in Fig. 1 are in relative photon units, normalized to 1.0 at 350 nm.

The flatter spectral response, i.e., a response that is less wavelength dependent, and greater sensitivity in the UV of quantum counters, as illustrated in Fig. 1, makes them more suitable for the determination of R correction values as a function of excitation wavelength than Si photodiodes, particularly below 300 nm. However, Si photodiodes do have the advantage of a wider wavelength range from about 250 nm to 1100 nm, making them preferred for general fluorescence applications, but less than ideal for EEM applications using UV excitation. The reported wavelength ranges for optimal performance of these quantum counters is 250 nm to 600 nm for RhB and Rh101, and 200 nm to 400 nm for DPA.[20] Even though the Rhodamine dyes are outside their optimal range below 250 nm and we found them to be less sensitive than DPA, they still performed nearly as well as DPA with significantly greater sensitivity than the Si photodiode in the region from 200 nm to 250 nm.

The S correction profile (normalized to 1.0 at 450 nm in Fig. 3) shows a dramatic fall off in the detection system's responsivity at shorter emission wavelengths, with a five-fold increase in the S correction factor when moving from 350 nm to 300 nm. However, at longer wavelengths the response is fairly consistent, with correction factors equal to approximately 1.0 between 370 nm and 500 nm. This improvement in the detector response is partly caused by the proximity of the emission wavelengths to the blazing of the emission monochrometer (at 500 nm), resulting in lower signal loss through the system and, ultimately, a lower required correction factor. The R correction factor as a function of excitation wavelength (normalized to 1.0 at 375 nm in Fig. 3) shows a different trend than the smooth S correction profile. Instead, there are two locations along the excitation wavelength range that require comparatively large R correction factors, corresponding to the areas of low excitation lamp intensity (<240 nm) and lower

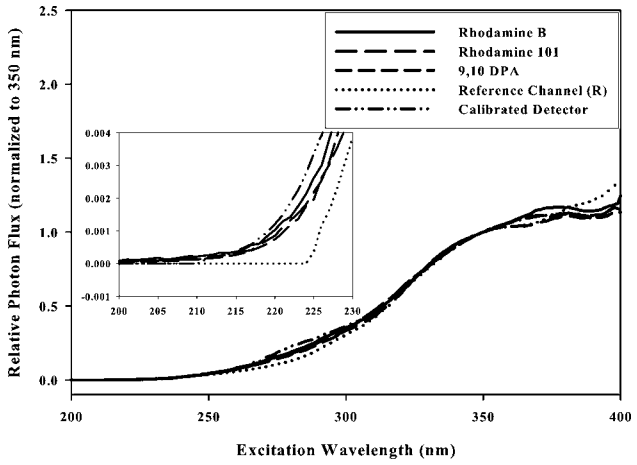

FIG. 1. Comparison of response from selected quantum counters, the reference channel (R), and calibrated detector as a function of excitation wavelength. Note that the fluorescence intensity is normalized at 350 nm to facilitate comparison.

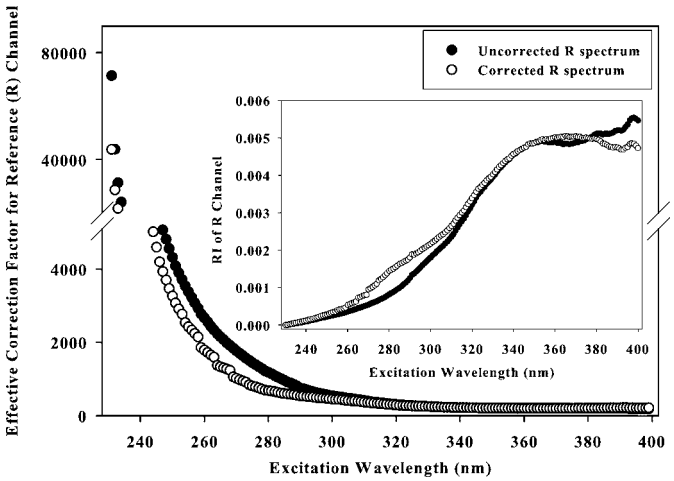

FIG. 2. Effective correction factor for corrected and uncorrected relative intensity of the reference (R) channel. Inset is the measured relative intensity (RI) of the R channel.

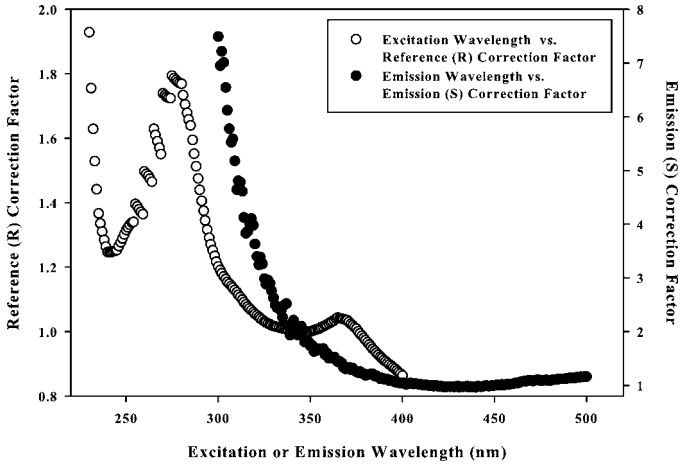

FIG. 3. Excitation correction factors as a function of excitation wavelength (open symbols and left ordinate, data normalized to 375 nm) and emission correction factors as a function of emission wavelength (filled symbols and right ordinate, data normalized to 450 nm).

than expected response of the Si photodiode (between 270 nm to 290 nm). However, the magnitude of the *R* correction factors is comparatively small, varying between 0.9 and 1.9, and lead to only slight differences between the uncorrected and corrected *R* spectrum (Fig. 2, inset). The effective correction factors for *R* are quite substantial in the low excitation wavelength region (<240 nm, Fig. 2), which correspond to the low energy output of the xenon lamp in this region.

Influence of Reference Intensity Normalization and Spectral Correction Factors. Raw EEMs collected directly from a fluorometer consist of multiple emission spectra that either have (e.g., *S*/*R*) or have not (e.g., *S*) been normalized to the reference intensity. This normalization may require manual selection (as with our instrument) or may occur automatically (in a manner unknown to the analyst). Similarly, application of the excitation and emission correction factors may either be manual or automatic. As with any instrument, it is imperative that one understands how the fluorescence intensity is being measured, corrected, and reported. Such awareness can save the scientist from making critical data collection and analysis errors. Our instrument can collect *either* raw *S or* raw *S*/*R* EEM data. Spectral correction factors are applied manually after complete EEM collection. This enables the entire range of errors that could be potentially made during EEM collection to be evaluated and quantified. When eliminating instrument bias, the two most critical errors that can occur are: (1) not correcting the emission spectra for differences in reference intensity (excitation energy) (Fig. 2), and (2) not applying the correction factors to the emission or excitation spectra (Fig. 3).

There are six possible combinations of fluorescence intensity measurements that can be obtained during EEM acquisition. They include the raw fluorescence emission intensity (*S*), the corrected fluorescence emission intensity (S_{cor}), the raw fluorescence emission intensity that has been normalized to the raw reference intensity (*S*/*R*), and various combinations of the later where correction factors have been applied to *S*, *R*, or both (S_{cor}/R, S/R_{cor}, and S_{cor}/R_{cor}, respectively). The resulting contour plots (Figs. 4A–4F) from the various EEM acquisition methods reveal substantial qualitative differences in surface features. (Note that the results for NAHA, SRFA, and SRNOM solutions were virtually identical to each other; only EEM plots of the biphasic NAHA and tryptophan mixture solutions are illustrated to facilitate presentation of the results.)

There are three expected peaks in the biphasic sample, two from the NAHA fluorophores (occurring at excitation/emission wavelengths pair of 240 nm/448 nm and 325 nm/452 nm, respectively) and one from tryptophan (280 nm/348 nm) for the excitation and emission ranges used in these experiments. However, there are no discernable fluorescence peaks below an excitation wavelength of 320 nm with a broad, almost featureless peak at 356 nm/456 nm when only *S* is collected (Fig. 4A). Application of the emission correction factor (S_{cor}, Fig. 4B) begins to reveal a small shoulder at approximately 290 nm/353 nm while the nearly featureless peak observed in Fig. 4A becomes more prominent but has a lower fluorescence intensity.

Surface features become apparent at lower excitation wavelengths when the fluorescence emission intensity is normalized to reference intensity with a third fluorescence peak being observed between 240 nm to 260 nm/440 nm to 460 nm (Figs. 4C through 4F, see below for discussion). The significant increase in fluorescence intensity at the lower wavelengths is caused by the large effective correction factors of the reference channel, which varies as a function of excitation wavelength (Fig. 2). The net result of reference intensity normalization is a substantial increase in fluorescence intensity between 230 nm to 270 nm, an almost linear increase between 270 nm and 340 nm, and little change between 340 nm and 400 nm. The large fluorescence intensity measurements at the lowest excitation wavelength (230 nm) in Fig. 4C are caused by the very low reference intensity values. Such spurious "peaks" are normally treated as noise and are removed from ensuing analysis. However, as illustrated below, such "peaks" can often be removed with proper use of the *S* and *R* correction factors.

The S_{cor}/R plot (Fig. 4D) retains the major features first observed in Fig. 4C, although a much more prominent fluorescence peak at 281 nm/353 nm and a less pronounced peak at 312 nm/415 nm are observed while there are no substantial peaks at longer excitation wavelengths. Application of the reference intensity correction factor to the raw fluorescence data (S/R_{cor}, Fig. 4E) leads to an excitation blue shift of the major fluorescence peak (241 nm/442 nm), a substantial reduction and emission red shift in the fluorescence intensity of the tryptophan peak (at 278 nm/375 nm), and a more pronounced peak at longer excitation wavelengths (331 nm/454 nm). However, it is not until both the *R* and *S* correction factors are applied to the reference intensity normalized EEM data that all three fluorescence peaks are clearly observed (S_{cor}/R_{cor}, Fig. 4F). Additionally, the spurious "peaks" at the lower excitation wavelengths are only minimally observed at lower emission wavelengths (between 300 nm and 360 nm).

Figures 4A through 4F clearly demonstrate the importance of correctly applying *R* and *S* correction factors to EEM data. A summary of the fluorescence peak locations and peak intensity biases for Figs. 4A through 4F is found in Table I, and serves to illustrate that correction factors are necessary to better resolve fluorescence peaks, define their true positions, and determine their peak intensity ratios. For example, there can be substantial red (+20 nm) and blue (−14 nm) excitation shifting as well as changes in the magnitude of the fluorescence intensity in the secondary peak when all correction factors are

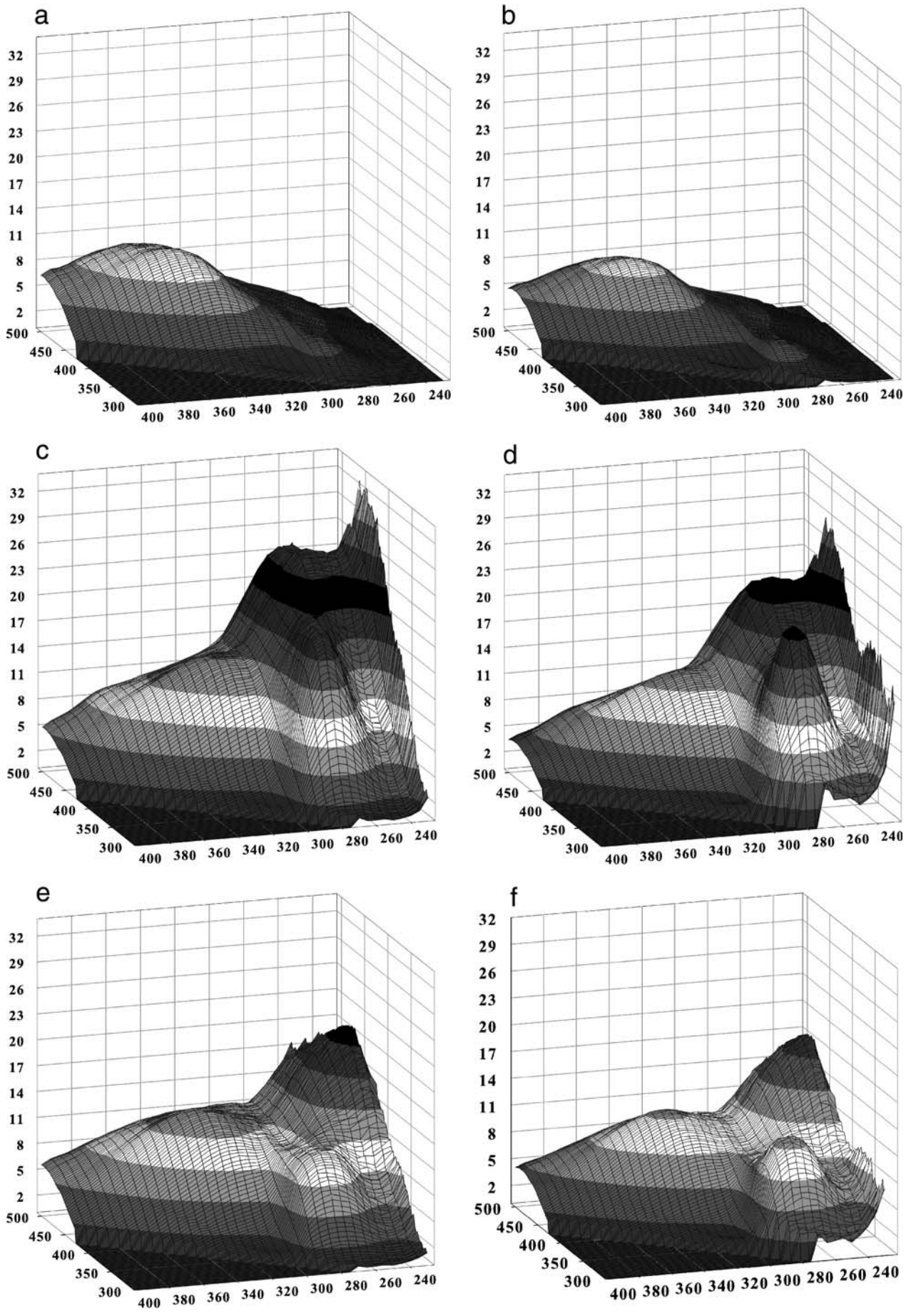
a
b
c
d
e
f
32
29
26
23
20
17
14
11
8
5
2
500
450
400
350
300
400 380 360 340 320 300 280 260 240

TABLE II. Comparison of fluorescence intensity differences (%) at specific excitation/emission wavelengths and characterization indices using various measurement and data handling procedures.[a]

Mixture	*S*	S_{cor}	*S/R*	S_{cor}/R	S/R_{cor}	S_{cor}/R_{cor}	Parameter
S		−8	**5353**	**4674**	**3957**	**3391**	Primary peak[b]
		−9	**61**	**36**	**53**	**29**	Secondary peak[c]
		36	**627**	**909**	**309**	**468**	Tertiary peak[d]
		−12	0	**−18**	1	**−17**	HI[e]
		15	1	**25**	1	**18**	FI[f]
S_{cor}			**5798**	**5063**	**4288**	**3676**	Primary peak[b]
			77	**49**	**68**	**42**	Secondary peak[c]
			433	**640**	**200**	**317**	Tertiary peak[d]
			14	−6	**15**	−5	HI[e]
			−12	9	**−12**	3	FI[f]
S/R				**−12**	**−26**	**−36**	Primary peak[b]
				−15	**−5**	**−20**	Secondary peak[c]
				39	**−44**	**−22**	Tertiary peak[d]
				−18	1	**−17**	HI[e]
				24	0	**16**	FI[f]
S_{cor}/R					**−15**	**−27**	Primary peak[b]
					12	**−5**	Secondary peak[c]
					−59	**−44**	Tertiary peak[d]
					23	1	HI[e]
					−19	−6	FI[f]
S/R_{cor}						**−14**	Primary peak[b]
						−15	Secondary peak[c]
						39	Tertiary peak[d]
						−18	HI[e]
						16	FI[f]

[a] Numbers reported are based on average of triplicate samples. Bold values denote a significant *p* value (student's t-test, $\rho < 0.05$).
[b] Fluorescence intensity from NAHA at 240 nm/446 nm.
[c] Fluorescence intensity from NAHA at 325 nm/452 nm.
[d] Fluorescence intensity from tryptophan at 280 nm/348 nm.
[e] Humification index.[10]
[f] Fluorescence index.[4]

not applied (Table I). The *S* correction factors are the most critical for low emission wavelength (between 300 nm and 350 nm) emitting fluorophore moieties, while the *R* correction factors are the most important for fluorophore fractions that absorb energy between 230 nm and 290 nm. Notably, fluorophores that both absorb and emit energy (e.g., tryptophan) or have weak fluorescence intensity signals within these wavelength ranges can be missed without proper spectral correction factors.

Quantitative Evaluation of Spectral Correction Factors on Excitation–Emission Matrix Data. The influence of spectral correction factors on intensity magnitude and physical location (described by excitation and emission coordinates), as well as characterization indices that can be calculated from EEM data, is discussed below.

Influence on Peak Fluorescence Intensities. The fluorescence intensity magnitude at specific excitation and emission wavelengths is significantly affected by the manner of data acquisition and application of spectral correction factors. This is best demonstrated by examining the data from the mixture of NAHA and tryptophan.

The three peak fluorescence intensity differences are summarized in Table II for the different data collection and handling procedures. For the primary and secondary peaks, the fluorescence intensity always decreases when the emission spectral correction factor is applied (such as the reduction that is observed when comparing *S* versus S_{cor} and *S/R* versus S_{cor}/R) by an emission correction factor less than unity for emission wavelengths less than 370 nm (Fig. 3). There is a significant increase in the fluorescence intensity once the emission intensity is normalized to reference intensity (i.e., *S/R*), with a slight reduction once the data is corrected for the excitation spectra (i.e., S/R_{cor}). This trend is caused by the large effective correction factors for the R channel with slight differences between the uncorrected and corrected spectrum (Fig. 2). The trends for the tertiary peak are a little different, with slight increases in the fluorescence intensity being associated with the emission spectral correction factor. This phenomenon is generally true of a fluorescence intensity whose emission wavelength is less than 370 nm (Fig. 3). Similar to the primary and secondary peaks, the tertiary peak intensity is much higher when corrected for the reference intensity.

Influence on Characterization Indices. Two characterization indices can be calculated from EEM data: the HI,[10] a relative measure of organic matter stability, and the FI,[4] which can be used to help identify the source(s) of organic matter (i.e., allochthonous versus autochthonous). Although these indices are strongly negatively correlated ($r = -0.87$, $n = 55$, data not shown), they are calculated using different excitation and emission wavelengths, and very small differences in the FI (on the order of 0.1 units) can be used to distinguish whether organic matter originated from microbial

←

FIG. 4. EEMs of mixture of Nordic aquatic humic acid and tryptophan using various measurement and data handling procedures. X-axis is excitation wavelength (230 nm to 400 nm), y-axis is emission wavelength (300 nm to 500 nm), and z-axis is fluorescence intensity (0 Raman units to 34 Raman units). (**A**) *S*; (**B**) S_{cor}; (**C**) *S/R*; (**D**) S_{cor}/R; (**E**) S/R_{cor}; and (**F**) S_{cor}/R_{cor}.

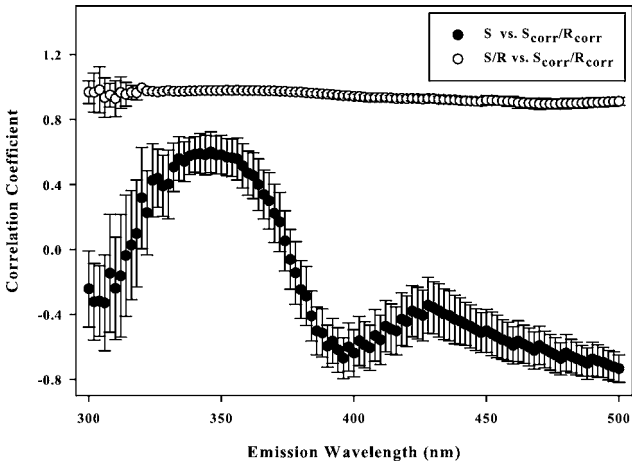

FIG. 5. Correlation coefficient plot of corresponding EEMs for mixture of Nordic Aquatic Humic Acid and tryptophan.

or terrestrial sources.[4] Consequently, it is important to understand how instrumentation bias may influence these indices in order to eliminate classification errors.

Because both indices are calculated as the ratio of single or range of emission wavelengths from a single excitation wavelength (254 nm for the HI[10] and 370 nm for the FI[4]), they are independent of the reference intensity. Normalization to the reference intensity or application of an excitation spectral correction factor will result in identical manipulation of both numerator and denominator, resulting in no net change of either index. For example, each index is virtually equivalent when either the emission intensity (S), the emission intensity normalized to the reference intensity (S/R), or the excitation spectral correction factor (S/R_{cor}) is compared (Table II). For proper quantification of the indices, only emission spectral correction factors are required. However, it is highly recommended that emission signals always be collected in ratio mode to account for both long and short time-dependent variations in such factors as lamp strength, temperature, and humidity.

Influence on Excitation and Emission Coordinates (Spectral Shape). Excitation and emission coordinates are often used to characterize aqueous environmental samples or to resolve distinct fluorophore moieties from complex mixtures.[2,21] A statistical analysis of the spectral shape for a given emission wavelength allows both visual (Fig. 5) and quantitative (Table III) evidence for significant fluorescence intensity shifts between different EEMs.

The analysis demonstrates that proper spectral shape can be strongly dependent on the use of a basic excitation spectral correction using an R channel, but is less influenced by either an emission spectral correction factor (S_{cor}) or an R correction factor (R_{cor}). Representative correlation plots are shown in Fig. 5 and illustrate that the coefficients were either consistently approximately equal to one or varied significantly as a function of the emission wavelength. These plots reveal a substantial correlative dependence on emission wavelength for EEMs that have not been reference intensity normalized (i.e., S or S_{cor}) with correlation coefficients varying between −0.67 and 0.61. Negative correlation coefficients indicate a mirror-image relationship between the EEM surfaces, where one EEM surface can be visualized as concave and the other as convex for a given emission wavelength. By comparison, there was little variation in correlation coefficients for EEMs that had been normalized to the reference intensity (e.g., S/R and S_{cor}/R_{cor}). There is some variation (between 0.90 and 0.98) in the S/R versus S_{cor}/R_{cor} relationship that is not apparent in Fig. 5, but this is comparatively minor.

Correlation coefficients can be combined through their p-values by the Fisher statistic, which facilitates a determination of significant or non-significant differences between corresponding EEMs. The Fisher statistics are summarized in Table III for the different data analysis methods and fluorescence materials tested. As with the correlation plots, this summary indicates that reference intensity normalization is necessary to maintain accurate spectral shape. EEM data that consists of either corrected (S_{cor}) or uncorrected (S) fluorescence intensity are significantly different from any EEM data that has been corrected for reference intensity. Similarly, a comparison

TABLE III. Summary of calculated Fisher statistics for different data analysis methods and fluorescence materials.[a]

Translational differences	S_{cor}	S/R	S_{cor}/R	S/R_{cor}	S_{cor}/R_{cor}	Sample
S	na[b]	**3688–3696**	**3689–3696**	**3700–3716**	**3700–3716**	IHSS material[c]
	na[b]	**1840**	**1842**	**2629**	**1829**	Tryptophan
	na[b]	**3176**	**3176**	**3289**	**3289**	Mixture[d]
S_{cor}		**3688–3696**	**3689–3696**	**3700–3716**	**3700–3716**	IHSS material[c]
		1840	**1842**	**2629**	**1829**	Tryptophan
		3176	**3176**	**3289**	**3289**	Mixture[d]
S/R			na[b]	52–117	52–117	IHSS material[c]
			na[b]	12	37	Tryptophan
			na[b]	42	42	Mixture[d]
S_{cor}/R				52–117	52–117	IHSS material[c]
				12	37	Tryptophan
				42	42	Mixture[d]
S/R_{cor}				na[b]	52–117	IHSS material[c]
				na[b]	37	Tryptophan
				na[b]	42	Mixture[d]

[a] Highlighted values denote significant Fisher statistics ($p < 0.001$). The critical Fisher statistic for determining whether two matrices are significantly different for these datasets (with df = 202) is 270 for ($p < 0.001$).
[b] na = not applicable (i.e., perfect correlation due to simple mathematical scaling of one matrix compared to the other).
[c] Includes Fisher statistics for Nordic Aquatic Humic Acid (NAHA), Suwannee River Natural Organic Matter (SRNOM), and Suwannee River Fulvic Acid (SRFA).
[d] Mixture of NAHA and tryptophan.

between EEM data that has been normalized is not significantly different, even if excitation and emission spectral correction factors have been applied, and is a result of the similar shape of the uncorrected and corrected reference intensity spectrum (Fig. 2). Therefore, although application of the *R* correction factors does lead to slight difference in the peak location (Table I), the major surface features of EEM data are present after reference intensity normalization. It should be noted that the correlation for spectral shape analysis is scale and translation invariant and so cannot be used to evaluate uniform changes in fluorescence intensity (i.e., changes in the z-axis direction). Consequently, the Fisher statistic cannot be applied to compare EEMs that differ only in whether or not an excitation or emission spectral correction factor has been applied (e.g., S/R versus S_{cor}/R).

What is also apparent from Table III is the magnitude difference between the calculated and critical Fisher statistic value. The critical value determines whether or not two EEMs can be considered significantly different and is a function of the degrees of freedom (i.e., number of data points), the user-defined lower acceptable correlation coefficient (ρ_0), and the significance level (α). For our analysis, we chose to use values of $\rho_0 = 0.90$ and $\alpha = 0.05$, which correspond to a critical Fisher statistic of 270. Those EEMs that were significantly different had Fisher statistics between 1840 and 3696, an order of magnitude higher than the critical value. Similarly, EEMs that were considered not significantly different had Fisher statistics between 12 and 117, almost an order of magnitude below the critical value. So, while the critical Fisher statistic would change, the results summarized in Table III regarding significant/non-significant differences would continue to hold for any reasonable ρ_0 or z_α value. This observation provides additional verification that reference intensity normalization is critical in maintaining proper EEM surface contour shape.

CONCLUSION

The peak fluorescence intensities of IHSS materials and tryptophan were significantly influenced by the application of excitation and emission spectral correction factors and by the wavelength dependence of each correction factor. Humification and fluorescence indices were also influenced by excitation and emission correction factors but were independent of reference intensity normalization. Spectral shape (EEM surface contours) was dependent on normalization of the fluorescence intensity to the reference intensity but was not influenced by either excitation or emission spectral correction factors. Although some parameters are seemingly independent of the reference intensity, it is highly recommended that EEM measurements always be collected in ratio mode to account for both long and short variations in such factors as lamp strength, temperature, and humidity. Lastly, authors should be explicit in how excitation and emission spectral correction procedures were implemented in their investigations, which will help to facilitate intra-laboratory comparisons and data sharing.

ACKNOWLEDGMENTS

R.D.H. acknowledges financial support from the National Research Council/ National Institute of Standards and Technology Postdoctoral Research program. Certain commercial equipment, instruments, or materials are identified in this paper in order to adequately specify the experimental procedure. Such identification does not imply recommendation or endorsement by the National Institute of Standards and Technology, nor does it imply that the materials or equipment identified are necessarily the best available for the purpose.

1. A. Baker, Environ. Sci. Technol. **35,** 948 (2001).
2. P. G. Coble, Mar. Chem. **51,** 325 (1996).
3. W. Chen, P. Westerhoff, J. A. Leenheer, and K. Booksh, Environ. Sci. Technol. **37,** 5701 (2003).
4. D. M. McKnight, E. W. Boyer, P. K. Westerhoff, P. T. Doran, and D. T. Andersen, Limnol. Oceanogr. **46,** 38 (2001).
5. P. G. Coble, C. E. Del Castillo, and B. Avril, Deep-Sea Res., Part 2 **45,** 2195 (1998).
6. R. D. JiJi, G. G. Andersson, and K. S. Booksh, J. Chemom. **14,** 171 (2000).
7. J.-P. Croué, G. V. Korshin, and M. Benjamin, *Characterization of Natural Organic Matter in Drinking Water* 2000. AWWA Research Foundation and American Water Works Association.
8. J. J. Mobed, S. L. Hemmingsen, J. L. Autry, and L. B. McGown, Environ. Sci. Technol. **30,** 3061 (1996).
9. S. A. Green, F. M. M. Morel, and N. V. Blough, Environ. Sci. Technol. **26,** 294 (1992).
10. T. Ohno, Environ. Sci. Technol. **36,** 742 (2002).
11. J. W. Hofstraatand and M. J. Latuhihin, Appl. Spectrosc. **48,** 436 (1994).
12. P. G. Coble, K. Mopper, and C. S. Schultz, Mar. Chem. **41,** 173 (1993).
13. R. Bro, Chemom. Intell. Lab. Syst. **38,** 149 (1997).
14. C. A. Stedmon, S. Markager, and R. Bro, Marine Chem. **82,** 239 (2003).
15. B. C. MacDonald, S. J. Lvin, and H. Patterson, Anal. Chim. Acta **338,** 155 (1997).
16. P. C. DeRose, E. A. Early, and G. W. Kramer, paper in preparation (2006).
17. B. Efron and R. J. Tibshirani, *An Introduction to the Bootstrap* (Chapman and Hall, New York, 1993).
18. E. L. Lehmann, *Testing Statistical Hypotheses* (John Wiley and Sons, New York, 1986).
19. J. R. Lakowicz, *Principles of Fluorescence Spectroscopy* (Kluwer Academic/Plenum Publishers, New York, 1999).
20. L. F. V. Ferreira, S. M. B. Costa, and E. J. Pereira, J. Photochem. Photobiol., A **55,** 361 (1991).
21. C. A. Stedmon and S. Markager, Limnol. Oceanogr. **50,** 686 (2005).